
Optimal Decentralized Voltage Control for Distribution Systems with Inverter-Based Distributed Generators

Sunkara Venkata Sirishnadh & Mr. P Victor

M.Tech (EEE), Department of Electrical & Electronics Engineering, Helapuri Institute of Technology and Science, Eluru, A.P.

Assistant Professor, Department of Electrical & Electronics Engineering, Helapuri Institute of Technology and Science, Eluru, A.P.

Abstract

The increasing penetration of distributed generation (DG) power plants into distribution networks (DNs) causes various issues concerning, e.g., stability, protection equipment, and voltage regulation. Thus, the necessity to develop proper control techniques to allow power delivery to customers in compliance with power quality and reliability standards (PQR) has become a relevant issue in recent years. This paper proposes an optimized distributed control approach based on DN sensitivity analysis and on decentralized reactive/active power regulation capable of maintaining voltage levels within regulatory limits and to offer ancillary services to the DN, such as voltage regulation. At the same time, it tries to minimize DN active power losses and the reactive power exchanged with the DN by the DG units. The validation of the proposed control technique has been

conducted through a several number of simulations on a real MV Italian distribution system.

Nevertheless, the connection of DGs to DNs poses well-known technical challenges for the network management. Among them, voltage rise represents one of the main issues concerning DG integration into DNs, especially in the case of nonprogrammable RES-DGs (e.g., wind- or solar-based ones) in weak DNs, characterized by a small value of reactance versus resistance ratio. Thus, the necessity to develop proper control techniques to ensure power delivery to customers in compliance with PQR requirements and to furnish ancillary services to the network is becoming a relevant issue

Introduction

The penetration of distributed generation power plants (DGs) into distribution networks (DNs) is rapidly increasing across the world in recent years. Various incentive programs have encouraged the adoption of renewable energy sources (RES)-based DGs in order to achieve the ambitious governments targets related to the promotion of a more sustainable development in the energy sector. For example, in 2009 the European Community (EC) has officially recognized

the need to promote RES as a priority measure. Furthermore, a significant increase of RES units within the EC and through the world is expected in upcoming years.

Nevertheless, the connection of DGs to DN's poses well-known technical challenges for the network management . Among them, voltage rise represents one of the main issues concerning DG integration into DN's, especially in the case of nonprogrammable RES-DGs (e.g., wind- o solar-based ones) in weak DN's, characterized by a small value of reactance versus resistance ratio. Thus, the necessity to develop proper control techniques to ensure power delivery to customers in compliance with PQR requirements and to furnish ancillary

services to the network is becoming a relevant issue.

It is possible to distinguish two main categories through the various approaches proposed to face DGs integration issues: centralized and decentralized control strategies. The first have

been extensively investigated by the scientific community . However, the application of centralized control strategies to the existing networks faces several drawbacks: in addition to the heavy investments necessary for devices and control systems, all centralized approaches require a highly reliable communication channel through the overall DN . For these reasons, the second category is gaining relevant interest in recent years. The adoption of decentralized approaches allows the DGs to provide ancillary services to the DN, such as reserves and voltage support . Moreover, it can have positive effects on both loss minimization and increased generation capacity because of their flexibility .

REACTIVE/ACTIVE POWER CAPABILITY OF INVERTER-BASED DG'S

Typically, RES-DGs are connected to the DN's by means of electronic power

converters. Among the decentralized control approaches, the capability of performing distributed control actions taking into account the converters reactive and/or active power controllable domains has recently been investigated. Such an approach could be useful to regulate voltage profiles and/or to offer ancillary services to the DN, maximizing active power production at the same time. In order to define the characteristics of the overall methodology presented within the paper, the structure of the proposed control system applied to a generic schematic diagram of an inverter based RES-DG is depicted in Control system structure represents the core of the OSAB-DC system and can be implemented on the on-board intelligence of each RES-DG plant connected to the DN by means of electronic converters. and are used by the OSAB-DC algorithm to perform the local control action. Concerning the inverter-based DG, the converter voltage depends on the dc-link voltage and the parameters of the adopted modulation technique. The reactance represents the total reactance of the transformers and grid filters used for the DG connection to the DN.

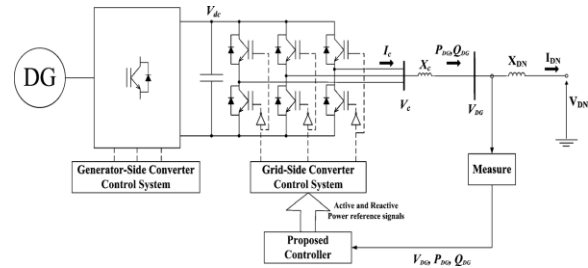


Fig. 5.1. Control system structure.

Starting from the maximum power supplied by the primary source (e.g., PV array, wind turbine), the converter current and voltage limits impose circular constraints to the DG capability to vary and [21]. From the equations necessary to compute and it is possible to write

$$\begin{cases} P_{DG} = V_{DN} I_{DN} \cos \theta \\ Q_{DG} = (V_{DN} \sin \theta + X_{DN} I_{DN}) I_{DN} \end{cases}$$

Taking into account the root mean square of the converter voltage as follows:

$$v_c = \sqrt{V_{DN}^2 + 2(X_{DN} + X_C) I_{DN} V_{DN} \sin \theta + (X_{DN} + X_C)^2 I_{DN}^2}$$

and, working on the equations, the following can be stated:

$$\left(\frac{X_C - X_{DN}}{X_C + X_{DN}} \right)^2 P_{DG}^2 + \left(Q_{DG} + \frac{2X_C V_{DN}^2 - X_{DN} V_C^2}{2(X_C + X_{DN})^2} \right)^2 < \left(\frac{(X_{DN} - X_C) V_C V_{DN}}{\sqrt{2}(X_C + X_{DN})^2} \right)^2$$

Since in almost all power systems applications is significantly greater than the DN feeder inductance, it is possible to compute the first circular constraint due to

the converter voltage , as stated by the following equation [22]:

$$P_{DG}^2 + \left(Q_{DG} + \frac{V_{DG}^2}{X_C} \right)^2 \leq \left(\frac{V_C V_{DG}}{X_C} \right)^2$$

With an analogous approach, it is possible to prove that the circular constraint imposed by the converter current is

$$P_{DG}^2 + Q_{DG}^2 \leq (V_{DG} I_C)^2$$

In order to evaluate the controllable domain of the DG it is necessary to take into account the converter's and values. Thus, the reactive versus active power constraints can be written as [21]

$$Q_{DG}^c = \sqrt{(V_{DG} I_{c,max})^2 - P_{DG}^2}$$

$$Q_{DG}^v = \sqrt{\left(\frac{V_{c,max} V_{DG}}{X_c} \right)^2 - P_{DG}^2} - \frac{V_{DG}^2}{X_c}$$

For each working point, the boundary of reactive power deviation available for the control action must be contained within the capability curve defined by

$$Q_{DG} = \min \{ Q_{DG}^c, Q_{DG}^v \}$$

Fig. 5.2 shows the capability curves for different PF values, whereas % 1.05 p.u., 0.95 p.u., and 1.01 p.u, [21]. To better explain the meaning of the curve it is possible to say that, e.g., for each value of the available and each value of the admitted PF, there are upper and lower limits to the

capability of varying . The upper and lower points on the curve in the figure represent these limits. Since the controllable domain equations mainly concern the grid-side converter model, this approach can be used for either full power back-to-back converter-connected WDGs and single- or double-stage inverter-connected PVs.

5.1. Sensitivity analysis-based-DC

The proposed controller performs a Sensitivity analysis-based-DC strategy by local control of reactive and/or active power exchange between each DG and the DN at the DG connection bus. Sensitivity analysis can be very useful to evaluate the relationships among voltage profiles changes and values necessary to implement a correct control action. In fact, sensitivity coefficients give information concerning the variation in the output of a model can be apportioned, qualitatively and quantitatively, to different sources of variation. Thus, they are very useful to predict or to face losses, bus voltages, and Within the paper, the sensitivity coefficients are computed only for the DN buses where DGs are connected. The evaluation of voltage versus reactive power sensitivity coefficient is implemented by fixing all DN parameters, including the

load and the generation profiles. At each time step, only the reactive power of each bus where the sensitivity parameters must be calculated is varied in turn, as stated in [10]. The voltages at each bus are recorded at each step, and then the sensitivity coefficients are computed. An analogous procedure is used to calculate the voltage versus active power sensitivity coefficients. Thus, if time step represents the system measurement time step, for each DG, it is possible to state that

$$\begin{cases} \Delta V_{DG}^Q(k) = \Delta Q_{DG}(k) / \rho_Q \\ \Delta V_{DG}^P(k) = \Delta P_{DG}(k) / \rho_P \end{cases}$$

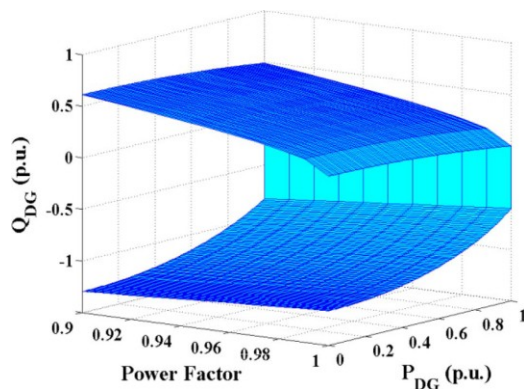


Fig. 5.2. DG capability curves.

Taking into account the relationships among voltage variations and reactive/active power variations stated in (8), the proposed SAB-DC can be defined. It is focused on maintaining voltage levels within regulatory

limits and avoiding, as much as possible, the DG disconnection. Its peculiarity is that the control action starts only if the voltage reaches warning values, defined by the introduction of two threshold levels placed around the nominal voltage value (1 p.u.). Two operational ranges are defined within the allowed range (AR): the operative range (OR) and the control range (CR) as depicted in Fig. 5.3. The control operations begin only if the DG bus voltage level enters the CR, causing a violation of the OR limits. More precisely, when the voltage value enters the CR, a certain amount of reactive and/or active power is injected/absorbed proportionally to the difference between the voltage value within the AR and the threshold value placed between the CR and the OR. The proportionality terms are represented by the sensitivity coefficients as in (8). To better explain the operation of the SAB-DC, the control algorithm flow chart in the case of upper threshold violation is shown in Fig. 5.4.

At the generic time instant, the procedure begins evaluating the difference between and the threshold value, as follows:

$$\Delta V_{DG}(k) = V_{DG}(k) - (V_{DG,max} - \epsilon_u)$$

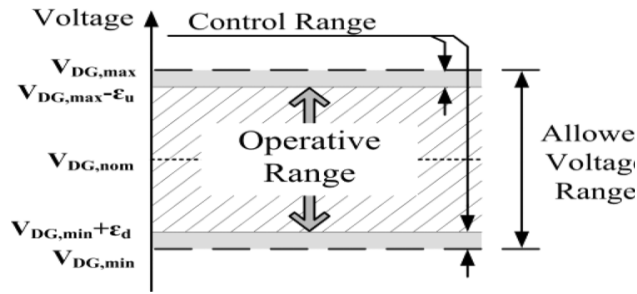


Fig. 5.3. Allowed, operative, and control ranges for the SAB-DC.

The control strategy considers related to injection/absorption by

$$\Delta V_{DG}(k) = \Delta V_{DG}^Q(k) + \Delta V_{DG}^P(k).$$

If reactive power injection is contained within the capability region of the DG converter and the voltage value is in the upper CR, the control system tries first to compensate the entire amount of voltage variation by increasing reactive power injected into the DN. Thus, the amount of to be varied is computed as

$$\Delta Q_{DG}(k) = \Delta V_{DG}(k) \cdot \rho_Q.$$

The maximum amount of used to bring back voltage levels within the OR is limited by the DG capability coverage . For each working point, represents the maximum value of reactive power that the converter is able to absorb and/or inject into the DN. Therefore, the DG reactive power is chosen according to (7) to yield

$$Q_{DG}(k) = \max \{ Q_{DG_cap}(k), Q_{DG}(k-1) - \Delta V_{DG}(k) \rho_Q \}$$

Then, only if is not capable of maintaining the voltage within the OR, an active power curtailment has to take place. The necessary amount is evaluated according to (8) and (10) as follows:

$$\Delta P_{DG}(k) = - \left[\Delta V_{DG}(k) - \frac{\Delta Q_{DG}(k)}{\rho_Q} \right] \cdot \rho_P.$$

This active power curtailment allows to decrease voltage levels and to obtain a higher reactive power injection capability because the working point is moved leftmost on the capability curve. The right part of the flowchart depicts the SAB-DC in the case of DG bus voltage contained within the OR. If a control action has been previously performed, the SAB-DC tries to recover at its maximum available value and to reduce the exchanged with the DN. Thus, is modified according to

$$P_{DG}(k) = \min \{ P_{DG_maxavail}(k), P_{DG}(k-1) - \Delta V_{DG}(k) \rho_P \}$$

Furthermore, if is below the active power amount proportional to , the residual voltage variation is used to reduce reactive power injection into the grid

$$\Delta Q_{DG}(k) = - \left[\Delta V_{DG}(k) - \frac{P_{DG_maxavail}(k) - P_{DG}(k-1)}{\rho_P} \right] \cdot \rho_Q.$$

to reduce the risk to be trapped in local minima compared with classical optimization strategies. Furthermore, these methods have been proved to be very suitable to solve nonlinear nonconvex problems like the one addressed within the paper. In fact, AI-based approaches have been proved to be more useful of other ones in which the threshold estimation was based on uncertainties evaluations . To drive an effective optimization procedure it is fundamental to obtain threshold values by applying them to a sample composed by variable generation and load demand profiles, assuring the coverage of a wide range of working conditions. In particular, DGs thresholds are computed by solving a multi-objective optimization problem based on the definition of two objective functions:

- reactive power objective : it tends to control the reactive power flow through the DN. It could be useful to improve voltage profiles, to allow high PF levels and to reduce power losses;
- power losses objective : it could help to increase system efficiency and decrease power generation cost. More precisely, the objective functions are computed as follows:

$$f_{Q_{DG}} = \sum_{i=1}^{N_G} \sum_{k=1}^K |Q_{DG}^i(k)|$$

$$f_{loss} = \sum_{j=1}^{N_B} \sum_{k=1}^K |P_j^{loss}(k)|.$$

The optimization problem is implemented on an overall time interval . It consists of optimal thresholds computation, aimed at minimizing the two objective functions. Thus, the overall optimization problem formulation results in

$$\min_{\underline{\varepsilon}} \{f_{Q_{DG}}, f_{loss}\}$$

$$\underline{\varepsilon} = \{\underline{\varepsilon}_1, \underline{\varepsilon}_2, \dots, \underline{\varepsilon}_{N_G}\}$$

where (20) defines the threshold matrix containing the threshold values of each DG controller. An approach based on multi-objective genetic algorithm (MOGA) interacting with a daily power-flow routine is performed to solve the optimization problem (19). The power flow routine is applied to daily generation and load demand profiles in order to maintain the problem formulation as much general as possible. Typical MOGA operators like elitism, selection, crossover, and mutation are taken into account. Several simulations with different MOGA operators are conducted in order to prove the validity of the proposed

approach. For each power-flow routine iteration, the optimization problem is subject to the following system operating constraints.

- Constraints applied to voltage levels, power factor, and reactive and active power capabilities of DGs:

CIRCUIT DESCRIPTION AND ANALYSIS

In order to prove the validity of the proposed OSAB-DC, a real Italian radial DN has been used. The single-line diagram of the DN is depicted in Italian radial DN under test.

It consists of a 20-kV distribution system fed by a 132-kV, 50-Hz sub transmission system with a short-circuit level of 750 MVA through a 150/20-kV /Yg transformer with rated power 25 MVA, %, and . The primary substation transformer's tap is fixed to 1.006 p.u., as one of the two classical strategies used in Italian distribution systems . The sensitivity coefficients have been evaluated according to the procedure stated in Section IV. Due to the offline procedure, several computations have been performed for various generation and loads values. Even if a very relevant change among the

sensitivity coefficients over the various computations is not observed, those calculated for the worst case scenario have been chosen for the SAB-DC optimization phase.

At the beginning of the simulations, the power factor has been set to 1. The maximum voltage variation of % around the nominal value has been imposed as stated in. The application of the optimization strategy to the network has been simulated running the MOGA in interaction with a power-flow routine based on daily generation and load forecasting, computed on a 10-min base in order to assure assessment of the state changes. Two different DGs penetration scenarios applied to the DN under test have been supposed in order to obtain a general validation of the proposed strategy. In Scenario A, four WDGs have been connected to the DN. In Scenario B, four PVs have been added to the previously defined scenario. The connection buses are highlighted in Fig. 6.1 and Table I, where the rated power values of the DGs are specified. The same rated power has been supposed for the WDGs, while two different configurations have been used for the PVs due to the modular characteristic of PV

plants. Fig. 6.2 shows the generation power profiles for WDGs and PVs and load demand for three different load types: residential, commercial, and industrial sectors. Without loss of generality and due to the upper OR infringement shown in Fig. 6.3 for both scenarios, the optimization strategy has been run to calculate only the upper thresholds. Thus, several simulations of the optimization strategy have been computed varying the MOGA parameters for each scenario, in order to investigate the assessment of the optimal solution.

validating the proposed methodology and the ones capable of assuring the optimal convergence of optimization procedure. As shown in the table, they correspond to ranges that assure a variability of the MOGA evolution that is not too excessive while preventing the premature ending of the simulation due to a minimum trap. Fig. 6.4 depicts the Pareto fronts of the optimal solution for both scenarios. It represents the tradeoff between the two conflicting objective functions. Each one of the points within the fronts represents a valid solution for the optimization problem. The controlled voltage values obtained using the solution that minimizes the reactive power objective function are shown in Fig. 6.5. It is worth noting that, in either scenario, the voltage values are contained within regulatory limits. Fig. 6.6 shows the reactive power injection into the DN by the DGs participating in the control actions. Scenario A concerns only the reactive power support from WDG connected at Bus 54, while Scenario B concerns the two WDGs connected at Buses 46 and 54 and the PV at bus 47. These DGs are those that enter the CR and infringe the voltage constraints in Fig. 6.3. It is worth noting a sort of sharing of the control action. In fact, the reactive

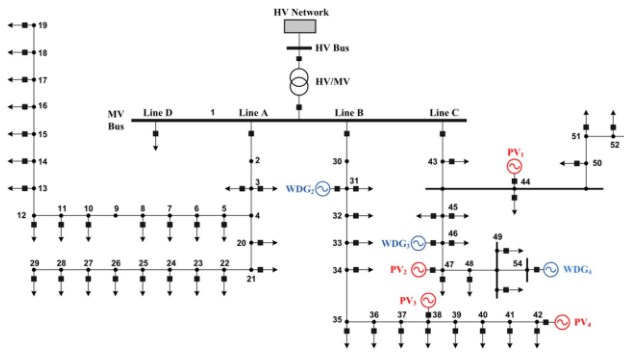


Fig. 6.1. Italian radial DN under test.

TABLE I: DGS RATED POWER AND PCC

Parameters		
DG	Rated Power (MW)	Connection Bus
WDG ₁ ÷ WDG ₄	2.5	53, 46, 54, 31
PV ₁ ÷ PV ₂	2.2	44, 47
PV ₃ ÷ PV ₄	1.4	38, 42

Table II shows the intervals adopted for the various MOGA parameters aimed at

power from WDG connected at bus 46 tends to compensate the feeder voltage boosting due to the end of the regulation action from WDG at bus 54 around the seventh operation hour.

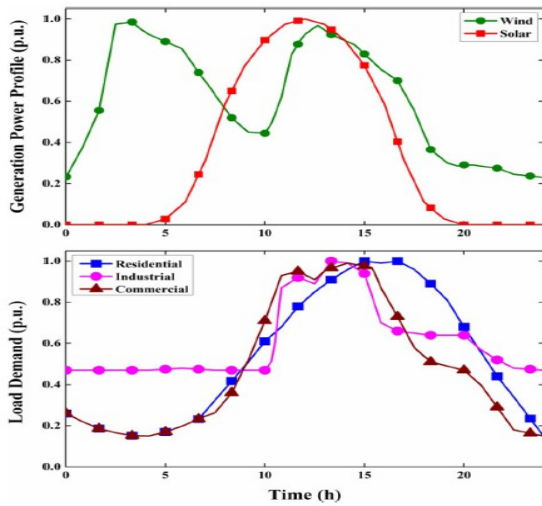


Fig. 6.2. Generation power profiles and load demand.

Fig. 6.6 shows the capability coverage of the proposed OSAB-DC for the DGs involved with the control action. The capability curve is computed from the equations in Section II. It represents the limit to the converter's capability to vary with respect to the available and the allowed PF range. The crosses in Fig. 6.6, Scenario A, represent the controller working points at each time step within the daily simulation interval.

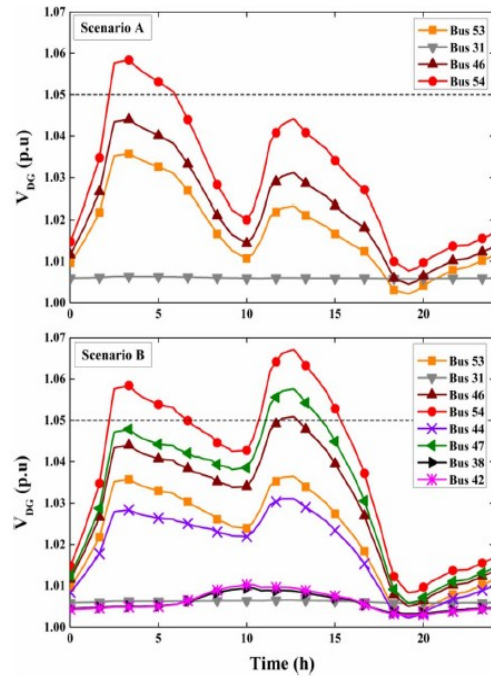


Fig. 6.3. DGs bus voltages without control action

TABLE II: MOGA VARIED PARAMETERS AMONG THE VARIOUS TESTS

Parameter	Test Range	Optimal Range
Crossover fraction	0.3÷0.9	0.4÷0.6
Migration Fraction	0.3÷0.9	0.4÷0.6
Elite Count	3÷20	3÷20
Population Size	50÷200	100÷200
Mutation Function	Uniform - Gaussian	Gaussian
Max Generation Number	100÷1000	400÷1000
Stall Generation Limit	100÷1000	400÷1000

Similarly, the points in Fig. 6.6, Scenario B, show the daily working points of each one of the OSAB-DC controllers that infringe the OR limits giving rise to the reactive/active control action. It can be stated that the optimized control action does

not require any curtailment of the available active power because of the absence of any capability curve constraint infringement. Thus, maximum available active power delivery is allowed by the proposed control strategy at a local level.

Furthermore, a different wind generation power profile has been applied to the WDG controllers optimized for the first case study in Scenario B in order to assess the robustness of the proposed solution, e.g., to unpredicted forecasting errors. Fig. 6.8 depicts the generation power profiles. Load demands have been maintained the same as in the previous example. Fig. 6.9 shows the worsening of the uncontrolled voltage profiles and the correct action performed by the OSAB-DC. As depicted in Fig. 14, the control action is maintained within the capability coverage of the DGs even in this case. Obviously, the PF drops below 0.95 (approximately 0.948). This value has been considered to be acceptable due to the PF Italian requirements for DGs connected by means of electronic converters (to be maintained within the range). Taking into account more restrictive PF regulations, the control action necessary to avoid DGs disconnection could be performed by a curtailment of active power production

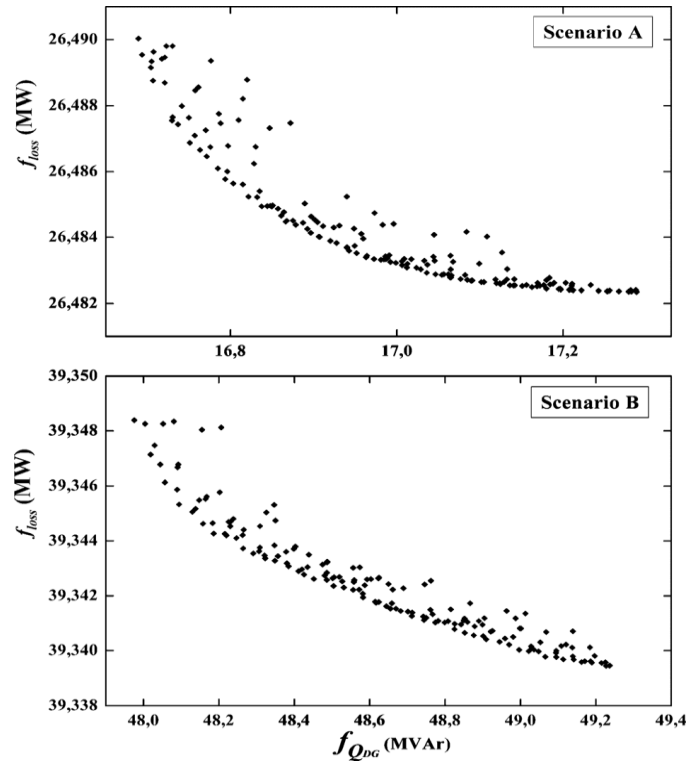


Fig. 6.4. Pareto fronts of the optimal solution.

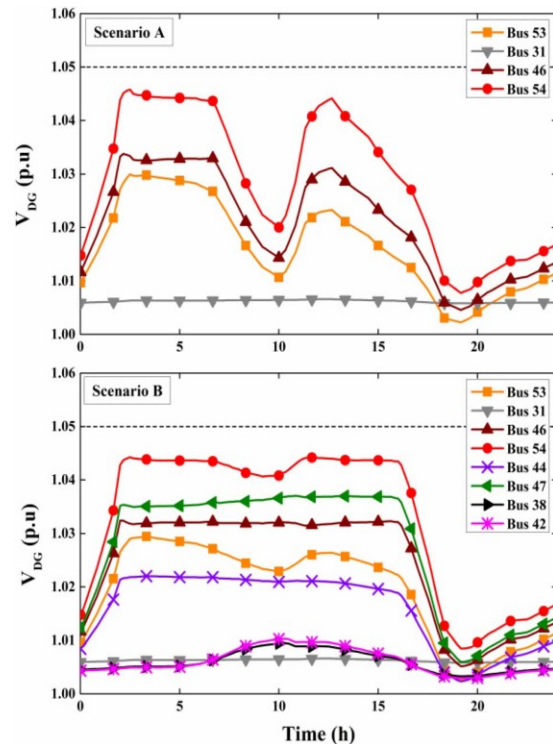


Fig. 6.5. Controlled voltage profiles.

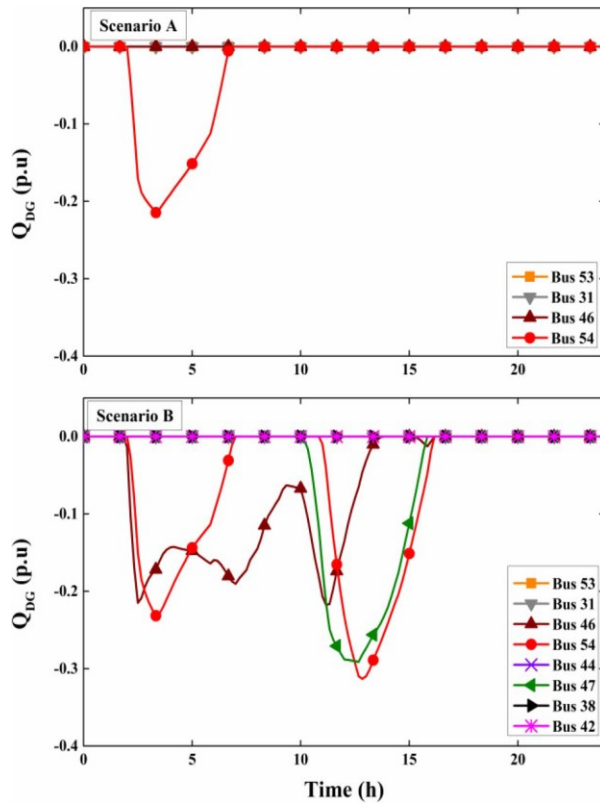


Fig. 6.6. Reactive power sharing among DGs.

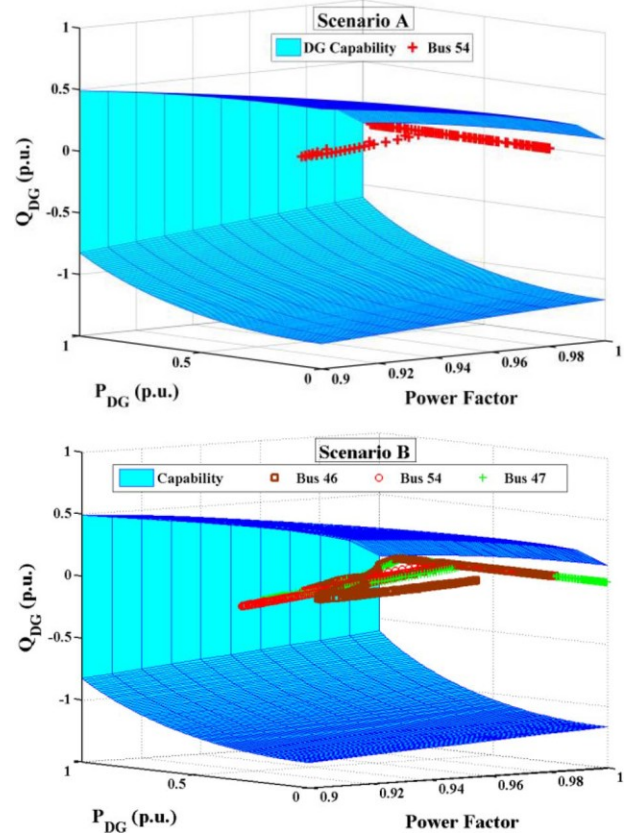


Fig. 6.7. Capability coverage of controlling DGs.

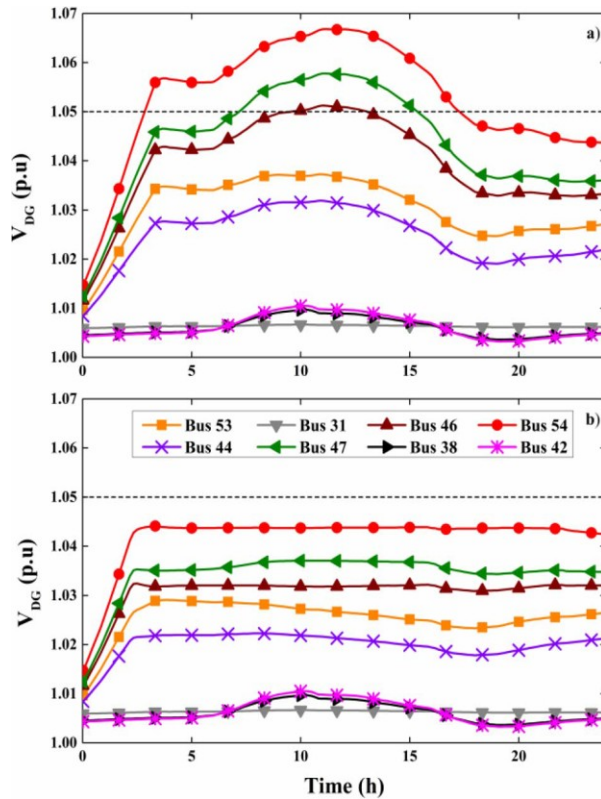
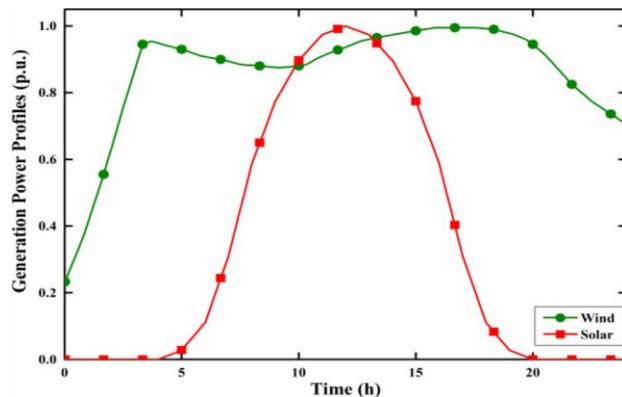


Fig. 6.8. DGs voltage profiles (a) Without control action enabled (b) With control action enabled.

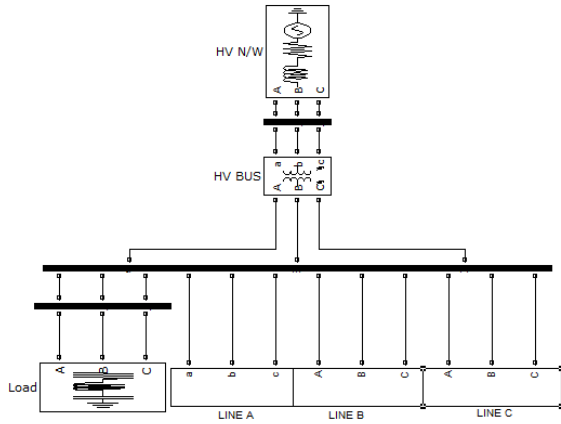


Modified wind generation profile for Scenario B.

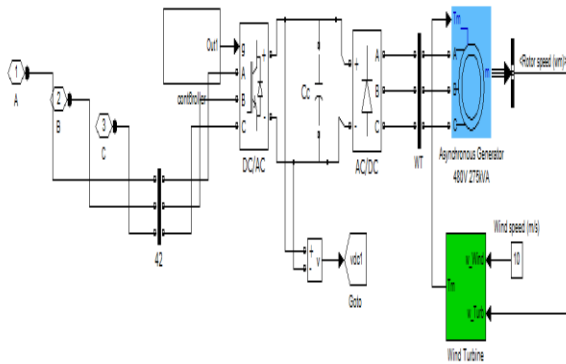
Considering that Scenario B represents the worst case among the two scenarios introduced previously, two further

optimization procedures are presented for this DGs integration scenario. Two different sets of generation and load profiles depicted in Fig. 6.11, concerning a Winter Weekday and a Summer Weekday, have been considered in order to prove the advantages of the proposed optimization methodology. Fig. 16 shows the uncontrolled voltage profiles at the DGs PCC for the two case studies. It is worth noting that the optimization procedure conducts to the calculation of thresholds capable of performing a correct control action for either of the case studies, as depicted in Fig. 6.13. Fig. 6.14 shows the reactive power contribution to the control action by each DG. For each case study, it is worth noting that the control action is performed by the DGs that infringe the AR, just as it did for the previous scenarios. Either the Winter and Summer Weekdays scenarios allow to perform a control action that avoid the DGs disconnection while maximizing active power production. It is important to point out that these control actions also take place without any active power curtailment

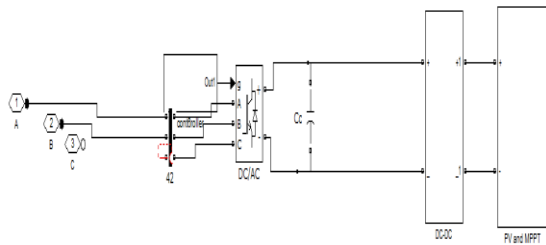
Italian Radial Distributed Network



Italian radial distributed network



Block Diagram Of Wind Power Generation



Block Diagram Of PV Power Generation

CONCLUSION

This paper has presented an optimization strategy applied to an SAB-DC for RES DGs, able to maintain voltage levels within regulatory limits while producing the maximum available active power. It avoids the DG disconnection due to violation of voltage limits at the connection bus and allows the DGs to offer ancillary services to the DN. A unified approach to the controller modeling in the case of RES DGs connected to the DN by means of electronic converters and the validity of the optimization strategy have been proposed and proved through several simulations run with different DGs penetration levels. All of the solutions presented by the Pareto fronts are valid thresholds for the optimization problem. The choice of one of them represents the optimal tradeoff between active losses and reactive power minimization. It could be useful for the distribution system operator (DSO) in order to determine the amount of the independent power producer (IPP) participation to the ancillary service operations. Thus, it allows to face the conflicting interests between DN losses minimization or reactive power action reduction aimed at maximum power production by the IPP. Results obtained by

the OSAB-DC application to different DGs scenarios have been shown. Its robustness with respect to unpredicted changes in generation power profiles has been proved through the simulations as well. This property allows reducing the communication channel reliability requirements that mainly concern only the optimized thresholds sharing and outages outages communications. No continuously detailed information is required to implement the correct control action. The OSAB-DC is well suited for large DG penetration cases due to its “local” nature that reduces the complexity of the control system compared with a completely centralized approach. It is characterized by a unified and modular configuration, and its simplicity and effectiveness would allow its practical implementation. In fact, its extension due to new DGs connections only requires, for example, that the DSO adds the capability specifications to the constraints section and two variables per each DG to the chromosome that represents the optimal solution to find. By run the MOGA on the DN model it would be possible to evaluate the optimal thresholds. Then, the online application of the OSAB-DC would be implemented by sensing voltage levels at the

DG connection bus. These features allow the OSAB-DC to be suitable for smart grid development scenarios because of its intrinsic modular and scalable architecture.

BIBLIOGRAPHY

- [1] “Directive 2009/28/EC of the European Parliament and of the Council,” *Official J. Eur. Union*, pp. 16–62, 2009.
- [2] Communication from the Commission to the European Parliament, the Council, the European Economic and Social Committee and the Committee of the Regions, “Energy roadmap 2050,” in *Proc. COM*, 2011, pp. 1–20.
- [3] Int. Energy Agency, “World Energy Outlook 2012, Executive Summary,” 2012, pp. 1–9.
- [4] R. A. Walling, R. Saint, R. C. Dugan, J. Burke, and L. A. Kojovic, “Summary of distributed resources impact on power delivery systems,” *IEEE Trans. Power Del.*, vol. 23, no. 3, pp. 1636–1644, Jul. 2008.
- [5] C.Masters, “Voltage rise the big issue when connecting embedded generation to long overhead 11 kV lines,” *Power Eng. J.*, vol. 16, no. 1, pp. 5–12, 2002.

[6] A. E. Kiprakis and A. R. Wallace, “Maximising energy capture from distributed generators in weak networks,” *Proc. Inst. Elect. Eng., Gen., Transm., Distrib.*, vol. 151, no. 5, pp. 611–618, 2004.

[7] E. J. Coster, J.M.A.Myrzik, B. Kruimer, and W. L. Kling, “Integration issues of distributed generation in distribution grids,” *Proc. IEEE*, vol. 99, no. 1, pp. 28–39, Jan. 2011.

[8] A. Casavola, G. Franzè, D. Menniti, and N. Sorrentino, “Voltage regulation in distribution networks in the presence of distributed generation: A voltage set-point reconfiguration approach,” *Electr. Power Syst. Res.*, vol. 81, pp. 25–34, 2011.